# Iron(II) Tris(3-bromo-1,10-phenanthroline) Complex: Synthesis, Crystal Structure and Electropolymerization

**Kyeong Jong Lee, Il Yoon, Shim Sung Lee, and Bu Yong Lee***

*Department of Chemistry and Research Institute of Natural Sciences, Gyeongsang National University, Chinju 660-701, Korea*
*Received September 1, 2001*

The complex of iron(II) tris(3-Br-phen) (3-Br-phen; 3-bromo-1,10-phenanthroline) was prepared as a precursor of electropolymerization and the crystal structure of $[Fe(3\text{-Br-phen})_3](PF_6)_2 \cdot CH_3CN$ with a distorted octahedral geometry has been investigated. The reductive electropolymerization of $[Fe(3\text{-Br-phen})_3]^{2+}$ complex onto the surface of a glassy carbon electrode and indium tin oxide (ITO) optically transparent electrode were performed in acetonitrile at room temperature. Thin film of poly-$[Fe(3\text{-Br-phen})_3]^{2+}$ formed was adherent, electroactive and stably deposited on a glassy carbon disk electrode. The thin metallopolymeric film formed was also confirmed by absorption spectroscopy.

**Keywords :** Electropolymerization, Poly-$[Fe(3\text{-Br-phen})_3]^{2+}$, Glassy carbon disk electrode, X-Ray crystal structure, Absorption spectroscopy.

## Introduction

Electropolymerization of a suitable ligand-complex onto the surface of an electrode has proven to be a most effective means to improve the application, selectivity and response properties of these surfaces.[1-5] Such chemically modified electrodes have found application in electrocatalysis,[6] electrochromic display,[7] solar energy conversion[8] and fabrication of electronic devices,[9] Much interest has been devoted to the formation of redox polymer films by electropolymerization of transition metal complexes containing vinly,[10] pyrroles,[11] thiophens[12] and amine groups,[13]

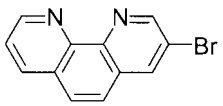


3-Br-phen

In our search for suitable electropolymerizable ligand-complex materials that could be useful in developing an application, 3-Br-phen was selected as a candidate ligand. The 3-Br-phen provides not only a readily reducible bromine moiety in the backbone of 1,10-phenanthroline but also a metal coordination site.

Here, we report the preparation of iron(II) complex of 3-Br-phen complex and its crystal structure together with the reductive electropolymerization of $[Fe(3\text{-Br-phen})_3]^{2+}$ and electrospectroscopic properties of the monomer and resultant thin film, poly-$[Fe(3\text{-Br-phen})_3]^{2+}$.

## Experimental Section

**Material**. Tetra-*n*-butylammonium hexafluorophosphate (TBAH, Aldrich, Milwaukee, Wisconsin, USA) was purified by a literature method.[14] Analytical grade acetonitrile was dried over molecular sieves (5 Å). 1,10-phenanthroline and other reagents for synthesis were purchased from Aldrich and used without further purification.

**Preparation of iron(II) tris(3-Br-phen) complex**. 3-Br-phen was synthesized by the procedure of Tor *et al.*[15] $Fe(NH_4)_2(SO_4)_2 \cdot 6H_2O$ (0.359 g, 0.916 mmol) and 3-Br-phen (0.264 g, 1.23 mmol) were dissolved in 50 ml of water with stirring and then heated mildly for 1 h. After cooling to room temperature, bright red product was precipitated by addition of an excess amount of $NH_4PF_6$. The solid product was filtered and dried under vacuum. Yield *ca.* 60% (Found C, 38.42; H, 2.19; N, 7.51. Calc. for $C_{36}H_{21}Br_3F_{12}N_6P_2$: C, 38.50; H, 1.88; N, 7.48%). IR (KBr disk, $\nu$/cm$^{-1}$): 3417, 3054, 2358, 1625, 1565, 1418, 1089. $^1$H NMR (acetone-$d_6$, 500 MHz) $\delta$; 9.09-9.07 (m, 3H), 8.86-8.83 (m, 3H), 8.48-8.45 (m, 3H), 8.40-8.36 (m, 3H), 8.31 (d, 1H), 8.27(d, 1H), 8.18 (d, 1H), 8.12 (d, 1H), 8.04-8.03 (m, 1H), 7.86-7.80 (m, 4H). $^{13}$C NMR ($CD_3OD$, 125 MHz) $\delta$; 158.54, 158.46, 158.22, 158.11, 158.09, 158.03, 157.70, 157.67, 150.67, 150.52, 150.48, 150.34, 149.60, 149.45, 149.26, 140.93, 140.86 (2C), 140.79, 138.92 (2C), 132.00, 131.96, 131.83, 131.71, 130.35, 128.33, 128.26 (2C), 127.60, 127.55, 127.49, 127.39, 121.55, 121.47, 121.36. FAB mass spectrum: *m/z* 415.95 and 416.93 for $[Fe(3\text{-Br-phen})_3]^{2+}$.

**X-Ray crystallography**. A crystal (size 0.02 × 0.20 × 0.30 mm) suitable for X-ray diffraction was mounted on a Siemens SMART diffractometer equipped with a graphite monochromated MoK$\alpha$ ($\lambda$ = 0.71073 Å) radiation source and a CCD detector, and 45 frames of two-dimensional diffraction images were collected and processed to deduce the cell parameters and orientation matrix. A total of 1271 frames of two-dimensional diffraction images were collected, each of which was measured for 30 sec. The frame data were processed to give structure factors by the program SAINT.[16] The intensity data were corrected for Lorentz and polarization effects. Using the program SADABS,[16] multi-scan ab-

sorption corrections were also applied. The structures were solved by a combination of the direct method and the difference Fourier methods provided by the program package SHELXTL,[17] and refined using a full matrix least square against $F^2$ for all data. All the non-H atoms were refined anisotropically. All hydrogen atoms were included in the calculated positions with isotropic thermal parameters 1.2 times those of the attached atoms. $C_{38}H_{24}FeN_7Br_3P_2F_{12}$, M = 1164.16, monoclinic red crystals (thin plate). Space group *P*2/c, $a$ = 19.654(4), $b$ = 11.727(2), $c$ = 18.093(4) Å, $\beta$ = 95.905(5)°, $Z$ = 4, $V$ = 4147.9(15) Å$^3$, $D_c$ = 1.864 Mg/m$^3$, $\mu$ = 3.425 mm$^{-1}$, F(000) = 2280. The final agreement factor was $R$ = 0.116 for 572 variables and 10204 unique reflections with I > 2$\sigma$(I). The relatively larger $R$-value even the repeated X-ray data collection is due to the small thickness (0.02 mm) of the platelet type of the crystals obtained.

**Electrochemistry**. Cyclic voltammograms were performed with a Bioanalytical Systems Model BAS 100 B/W voltammetric analyzer. Purified acetonitrile was used as a solvent. A supporting electrolyte for voltammetric measurements was 0.1 M TBAH. A glassy carbon disk electrode (0.071 cm$^2$, Bioanalytical Systems Co.) and optically transparent ITO electrode, that was cut from a large sheet (ITO; Hoya, 64 × 54 × 0.15 mm) into 8 × 20 × 0.15 mm were used as working electrodes, respectively. Before electropolymerization, ITO electrodes were treated by soaking for 30s in $CH_3CN$ and were dried. For all voltammetric measurements, a saturated Ag/AgCl electrode and platinum wire (diameter 0.5 mm) were used as a reference and a counter electrode, respectively. The glassy carbon electrode was mechanically cleaned before use with polishing alumina (Bio Analytical Systems Co.) and rinsed several times with acetone and acetonitrile. Thin films of poly-$[Fe(3\text{-Br-phen})_3]^{2+}$ were grown in $CH_3CN$ solutions containing 2.0 mM of monomer complex and 0.1 M TBAH by repeatedly cycling the potential of the working electrode between −0.7 and −1.8 V at a scan rate of 100 mV · s$^{-1}$. Two compartment electrochemical cells were used for electropolymerization. Before electropolymerization, dissolved oxygen was removed by purging with $N_2$ through the solutions for 15 min. The absorbance measurement of metallopolymeric film on the ITO electrode was made with a Hewlett-Packard Model-8453 UV-visible spectrophotometer.

## Results and Discussion

**Synthesis of iron(II) tris(3-Br-phen) complex, $[Fe(3\text{-Br-phen})_3](PF_6)_2$.** The reaction of $Fe(NH_4)_2(SO_4)_2 \cdot 6H_2O$ with 3-Br-phen followed by the addition of $NH_4PF_6$ in water afforded bright red solid product in reasonable yield. The FAB mass data of the product together with microanalysis are consistent with the formula. $^1$H and $^{13}$C NMR spectra of the complex in acetone-$d_6$ exhibit the non-equivalent 21 hydrogen and 36 carbon atoms, respectively, suggesting that the complex forms a distorted structure with 1 : 3 stoichiometric ratio (metal to ligand) in solution.

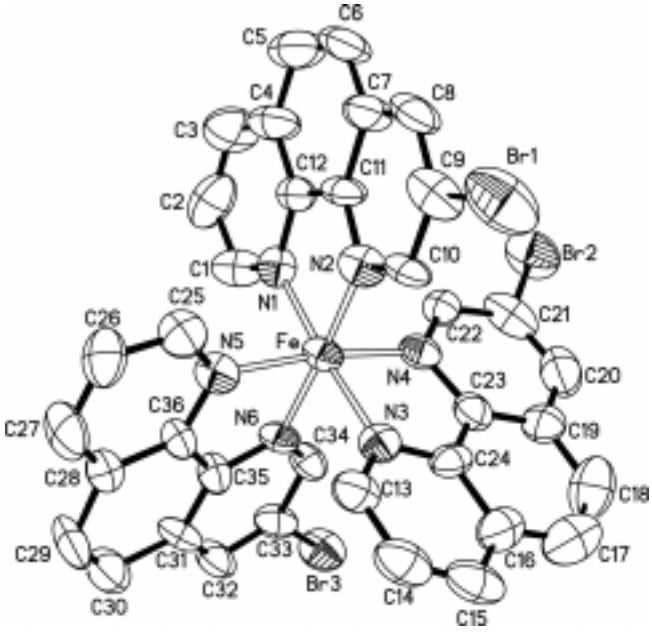


**Figure 1**. X-ray crystal structure of $[Fe(3\text{-Br-phen})_3]^{2+}$. The $PF_6^-$ ions, acetonitrile and H atoms are omitted for clarity. Displacement ellipsoids are shown at the 30% probability level.

**Crystal structure of iron(II) tris(3-Br-phen) complex**. X-ray diffraction of a single crystal is the most reliable method of establishing chemical structure. Unfortunately, metallopolymeric films are amorphorous, therefore unsuitable for single crystal diffraction studies. Thus, we prepared single crystals of monomeric species and characterized the crystal structure. The single crystals for X-ray analysis were grown as red platelets in acetonitrile solution by vapor diffusion of diethyl ether.

ORTEP drawing of the structure of the complex is presented in Figure 1. The complex consists of a mononuclear cation $[Fe(3\text{-Br-phen})_3]^{2+}$, two hexafluorophosphate ions and one acetonitrile. The potential symmetry of the complex cation may be broken by the substituted bromine atom, non-coordinating anion and solvent in the crystal. In the complex cation, the three 3-Br-phen molecules are coordinated to the central iron(II) atom through six nitrogen atoms to form a distorted octahedron, whose corresponding bonding distances

**Table 1**. Selected bond lengths [Å] and angles [°] for $[Fe(3\text{-Br-phen})_3](PF_6)_2 \cdot CH_3CN$

| | | | |
|---|---|---|---|
| Fe-N(1) | 1.960(10) | Fe-N(2) | 1.982(9) |
| Fe-N(3) | 1.987(10) | Fe-N(4) | 1.949(10) |
| Fe-N(5) | 2.007(10) | Fe-N(6) | 2.008(9) |
| | | | |
| N(1)-Fe-N(2) | 83.7(4) | N(3)-Fe-N(4) | 82.3(4) |
| N(5)-Fe-N(6) | 82.3(4) | N(1)-Fe-N(4) | 94.3(4) |
| N(1)-Fe-N(5) | 91.6(4) | N(1)-Fe-N(6) | 95.9(4) |
| N(2)-Fe-N(3) | 93.7(4) | N(2)-Fe-N(4) | 91.4(4) |
| N(2)-Fe-N(5) | 94.5(4) | N(3)-Fe-N(5) | 92.1(4) |
| N(3)-Fe-N(6) | 86.9(4) | N(4)-Fe-N(6) | 91.8(4) |
| N(1)-Fe-N(3) | 175.6(4) | N(2)-Fe-N(6) | 176.8(4) |
| N(4)-Fe-N(5) | 172.1(4) | | |

(Fe-N bonds; 1.96-2.01 Å) and bonding angles (N-Fe-N; 82-96° and 172-177°) agree with the similar system[18]. Selected bond distances and angles are given in Table 1. The anions and solvent molecule of the crystal are in the outer sphere of the complex (not shown).

**Electropolymerization from iron(II) tris(3-Br-phen) complex**. Figure 2a shows the consecutive cyclic voltammetry of the ligand region for $[Fe(3\text{-Br-phen})_3]^{2+}$ on a glassy carbon disk electrode in 0.1 M TBAH/$CH_3CN$ solution. A progressive increase in cathodic current near −1.5 V ($E_c$), which is characteristic of formation and interfacial accumulation of redox active polymeric material, is observed and the peak potential shifts to a more negative direction. This negative shift is believed to arise from bromine-carbon groups to the conversion of a single carbon-carbon coupling between the monomer units,[19] implying a loss of bromine substituent. From this negative shift of peak potential for the irreversible reduction wave in the first 5~6 scans, it can be inferred that reduction is followed by the rapid loss of $Br^-$ ion and formation of polymer. The release of $Br^-$ ion is shown by the appearance of the irreversible $Br^-$ oxidation waves upon initial several oxidation scans. The successive electropolymerization resulted the oxidation of $Br^-$ ion in the metal region between +0.8 ~ +1.20 V($E_a$).[19] Thus, the disappearance of the peak at −1.25 V with repetitive cycling is attributed to a progressive loss of adsorption sites due to the polymerization on the electrode surface. Removal of the electrode after several tens of cycles revealed a red film on the electrode surface that was retained during rinsing.

To measure surface coverage of deposited poly-$[Fe(Br\text{-phen})_3]^{2+}$ on glassy carbon electrode, further voltammetric measurements after transfer of the electrode to a solution without iron(II) complex were made. They showed that the film retained its electroactivity, which is attributed to the poly-$[Fe^{III/II}(3\text{-Br-phen})_3]^{2+}$ couple in the metal region (Figure 2b). Two successive cycles for $Fe^{III/II}$ couple were obtained (first cycle; $E_{1/2}$ = 1.26 V, second cycle; $E_{1/2}$ = 1.28 V). The first cycle, with an intense and broad signal, was due to the overlapping of the trapping peak[10] or shoulder for the oxidation of $Br^-$ to $Br_2$.[19,20] Anson *et al.*[21] observed similar shoulder peaks, which are due to the oxidation of $Cl^-$ by addition of tetraethylammonium chloride or NaCl to the working compartment solution of $[Ru(phen)_3]^{2+}$ near $E_a$ = +1.2 V (*vs.* SCE).

Figure 2c shows the cyclic voltammogram of the ligand region in a fresh electrolyte solution followed by electropolymerization. The sharp peak at −1.06 V (first scan) or 1.09 V (second scan) corresponds to the trapping peak[10]. The very small shoulders near 1.5 V are due to the irreversible reduction of the polymeric film.

To examine the effect of cycle number on the surface coverage ($\Gamma$), the cyclic voltammograms for the $Fe^{III/II}$ were carried out. The prepared electrodes were rinsed thoroughly with acetone after the electrochemical film formation and placed in a fresh electrolyte solution where the surface coverage ($\Gamma$) was determined electrochemically. The surface coverage was based on the area under the $Fe^{III/II}$ couple, without taking into account the charge due to trapping peak or shoulder of $Br^-$ oxidation. This was obtained by the charge (Q) under reductive wave of the specified metal redox peak ($Fe^{III/II}$) and by using equation (1), where *n* is the number of electrons per molecule reduced, *F* represents Faraday's constant, and A is the area of the working electrode in $cm^2$.

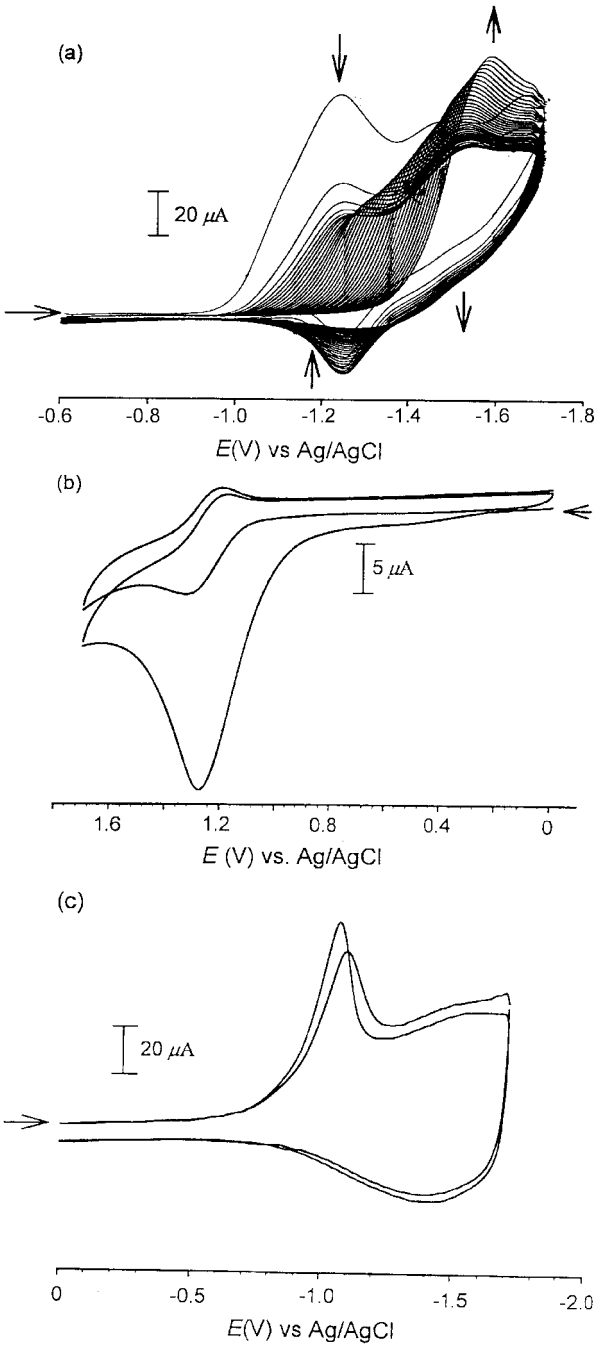


**Figure 2**. (a) Representative voltammograms of 2.0 mM $[Fe(3\text{-Br-phen})_3]^{2+}$ in 0.1 M TBAH/$CH_3CN$ at glassy carbon disk electrode. Scan rate; 100 mV · $s^{-1}$. (b) Cyclic voltammogram of $Fe^{III/II}$ couple of the poly-$[Fe(3\text{-Br-phen})_3]^{2+}$ film resulted from (a) in a fresh electrolyte solution. $\Gamma$; $1.50 \times 10^{-9}$ mole · $cm^{-2}$. Scan rate; 100 mV · $s^{-1}$. (c) Cyclic voltammogram of ligand region of poly-$[Fe(3\text{-Br-phen})_3]^{2+}$ film resulted from (a) in a fresh electrolyte solution.

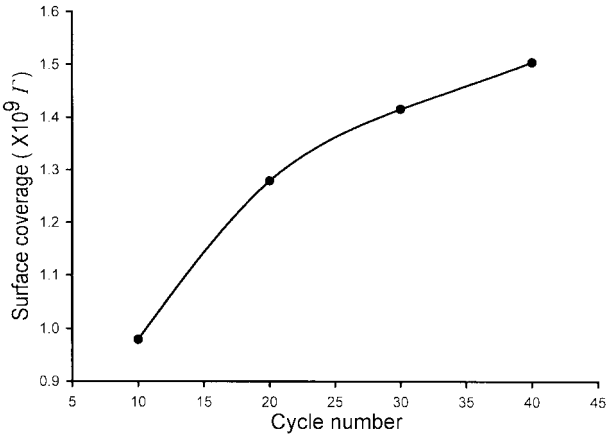


**Figure 3**. Plot of surface coverage ($\Gamma$) versus number of voltammetric cycle for poly-$[Fe(3\text{-Br-phen})_3]^{2+}$ film growth.

$$\Gamma = Q/nFA \quad (1)$$

Figure 3 shows how the surface coverage increased with an increasing number of electropolymerizing potential scans for $[Fe(3\text{-Br-phen})_3]^{2+}$. The polymer film growth is observed to occur nearly linearly for the first 20 cycles and less rapidly grow thereafter.

The electrochemical measurement observed for the monomeric complex consists of a ligand and metal center, respectively. A ligand-based wave (Figure 4a) and a reversible

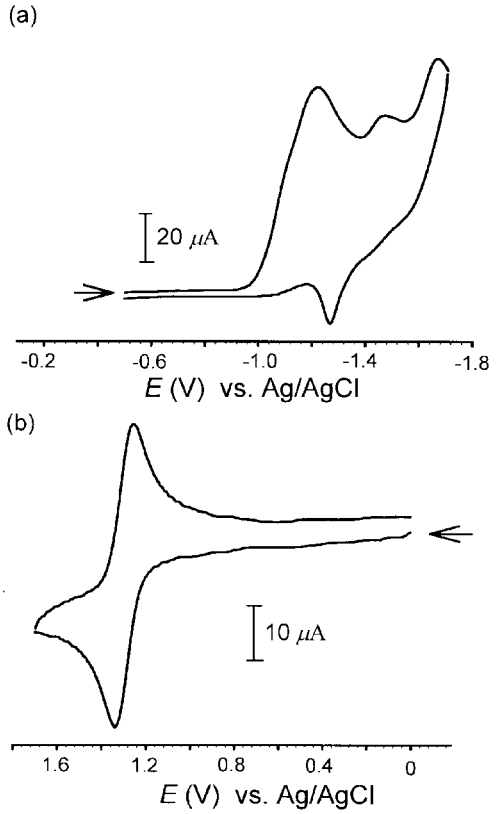


**Figure 4**. Cyclic voltammogram of (a) a ligand-based and (b) a reversible $Fe^{III/II}$ couple of monomeric $[Fe(3\text{-Br-phen})_3]^{2+}$ on glassy carbon electrode. Electrolyte solution; 0.1 M TBAH/$CH_3CN$. Scan rate; 100 mV · $s^{-1}$.

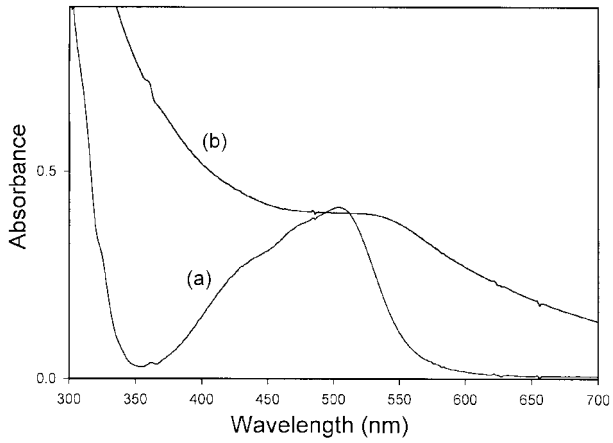


**Figure 5**. Absorption spectra of (a) $[Fe(3\text{-Br-phen})_3]^{2+}$ in $CH_3CN$ and (b) poly-$[Fe(3\text{-Br-phen})_3]^{2+}$ film on an optically transparent ITO electrode.

$Fe^{III/II}$ couple (Figure 4b, $E_{1/2}$ = 1.30 V) appear in the voltammogram of $[Fe(3\text{-Br-phen})_3]^{2+}$ simultaneously. During the electropolymerization procedure, the peak potentials of each species shifted. In practice, after polymerization, the irreversible peak of polymeric $Fe^{III/II}$ couple (Figure 2b) is shifted to a more negative potential ($\Delta E_{1/2}$ = *ca.* –30 mV) from that of the monomeric one (Figure 4b). The shift in potential is consistent with the replacement of an electronegative Br-C(aromatic) substituent by a more electron-rich C(aromatic)-C(aromatic) bond that links phenanthroline ligands.[20]

**Absorption spectra**. Accumulation of reductive product of $[Fe(3\text{-Br-phen})_3]^{2+}$on an ITO electrode made it possible to record the metal to ligand charge transfer (MLCT) absorption spectra in visible region. The absorption spectrum of poly-$[Fe(3\text{-Br-phen})_3]^{2+}$ film grown on an ITO electrode is compared with that of the monomer complex in $CH_3CN$ solution in Figure 5. The MLCT band of polymer (Figure 5b, $\Delta\lambda_{max}$ = 548 nm) is markedly shifted to a longer wavelength ($\Delta\lambda_{max}$ = 44 nm) from that of monomeric one (Figure 5a, $\lambda_{max}$ = 504 nm). Upon complexation, the red-shift of the maximum peak also suggests that the electropolymerizaton involves the bromine-carbon group and that the polymerization process converts them into the carbon-carbon groups.[22] In addition, the polymer peak is much broader than that of the monomer and the absorption tails to 700-800 nm. The broadening can be attributed to the interaction between the absorption sites in the polymer.

**Acknowledgement**. Authors acknowledge helpful discussion from Dr. Ki-Min Park for X-ray data.

## References

1. Murray, R. W. In *Molecular Design of Electrode Surfaces*: *Techniques of Chemistry Series*; Murray, R. W., Ed.; Wiley: New York, 1992; Vol. 22, p 1.
2. (a) Merz, A. In *Topics in Current Chemistry: Electrochemistry IV,* Steckhan, E., Ed.; Springer-Verlag: Berlin, 1990; Vol. 152, p 49. (b) Heinze, J. In *Topics in Current Chemistry: Electrochemistry IV,* Steckhan, E., Ed.; Springer-Verlag: Berlin, 1990; Vol. 152, p 1.
3. Josowicz, M.; Janata, J. In *Electroactive Polymers*, Scrosati, B.

Ed.; Chapman and Hall: New York, 1993; p 310.
4. Bedioui, F.; Devneck, J.; Bied-Charreton, C. *Acc. Chem. Res.* **1995**, *28*, 30.
5. Juris, A.; Balzani, V.; Barigelletti, F.; Campagna, S.; Belser, P.; von Zelewsky, A. *Coord. Chem. Rev.* **1988**, *84*, 85.
6. (a) Andrieux, C. P.; Saveant, J. M. In *Molecular Design of Electrode Surfaces*: *Techniques of Chemistry Series*; Murray, R. W., Ed.; Wiley: New York, 1992**,** Vol. 22, p 207. (b) Lyons, M. E. G. *Electroactive Polymer Electrochemistry*, 2nd Ed.; Plenum Press: New York, 1994; part 1 and references therein.
7. Monk, P. M. S.; Mortimer, R. J.; Rosseinsky, D. R. *Electrochromism: Fundamental and Applications*; VCH: Weinheim, 1995.
8. (a) Abruna, H. D.; Bard, A. J. *J. Am. Chem. Soc.* **1981**, *103*, 6898. (b) Moss, J. A.; Stipkala, J. M.; Yang, J. C.; Bignozzi, C. A.; Meyer, G. J.; Meyer, T. J.; Wen, X.; Lincton, R. W. *Chem. Mater.* **1998**, *10*, 1748. (c) Girotto, E. M.; Gazotti, W. A.; De Paoli, M. A. *J. Phys. Chem. B* **2000**, *104*, 6124.
9. Abruna, H. D.; Denisevich, P.; Umana, M.; Meyer, T. J.; Murray, R. W. *J. Am. Chem. Soc*. **1981**, *103*, 1.
10. Denisevich, P.; Abruna, H. D.; Leidner, C. R.; Meyer, T. J.; Murray, R. W. *Inorg. Chem.* **1982**, *21*, 2153.
11. Deronzier, A.; Moutet, J. C. *Coord. Chem. Rev.* **1996**, *147*, 339.
12. Wang, J.; Keene, F. R. *J. Electroanal. Chem*. **1996**, *405*, 71.
13. Belanger, S.; Stevenson, K. J.; Mudakha, S. A.; Hupp, J. T. *Langmuir* **1999**, *15*, 837.
14. Gould, S.; OToole, T. R.; Meyer, T. J. *J. Am. Chem. Soc*. **1990**, *112*, 9490.
15. Connors, P. J., Jr.; Tzalis, D.; Dunnick, A. L.; Tor, Y. *Inorg. Chem.* **1998**, *37*, 1121.
16. Siemens, *SMART and SAINT: Area Detector Control and Integration Software Ver. 4.0*; Siemens Analytical X-ray Instruments: Madison, Wisconsin, 1996.
17. Siemens, *SHELXTL: Structure Determination Programs Ver. 5.03*; Siemens Analytical X-ray Instruments: Madison, Wisconsin, 1996.
18. Zalkin, A.; Templeton, D. H.; Ueki, T. *Inorg. Chem.* **1973**, *12*, 1641.
19. Fussa-Rydel, O.; Zhang, H. T.; Hupp, J. T.; Leidner, C. R. *Inorg. Chem*. **1989**, *28*, 1533.
20. Gould, S.; Strouse, G. F.; Meyer, T. J.; Sullivan, B. P. *Inorg. Chem*. **1991**, *30*, 2942.
21. (a) Nguyen, F.; Anson, F. C. *Electrochim. Acta* **1998**, *44*, 239. (b) Redepenning, J.; Anson, F. C. *J. Phys. Chem*. **1987**, *91*, 4549.
22. Tzalis, D.; Tor, Y. *Tetrahedron Lett.* **1995**, *36*, 6017.